

10.1 EVALUATION OF THE HPAC DISPERSION MODEL WITH THE JOINT URBAN 2003 (JU2003) TRACER OBSERVATIONS

Steven R. Hanna¹, Joseph C. Chang², John M. White³, and James F. Bowers³

¹Hanna Consultants, Kennebunkport, ME; ²Fairfax, VA; ³U.S. Army Dugway Proving Ground, UT

ABSTRACT

Results are presented of a comprehensive evaluation of the Hazard Prediction and Assessment Capability (HPAC) model, using data from the Joint Urban 2003 (JU2003) Field Experiment in Oklahoma City. This paper focuses on Intensive Operating Periods (IOPs) 3 through 10, where the first four are during the daytime and the last four are during the nighttime. There were three separate continuous releases (of 30 minute duration) of SF₆ tracer each day from a point source near ground level, in or immediately upwind of the built-up downtown area. Tracer was sampled from over 100 locations at distances ranging from 0.1 to 4 km from the source. Two alternate urban configurations of HPAC are tested using four optional meteorological inputs. The two urban configurations are the Urban Dispersion Model (UDM) model and the Urban Canopy (UC) model. The four meteorological input options are basic default National Weather Service data (BDF), a single averaged wind over the domain (SGL), an upwind anemometer and radiosonde (UPWIND), and detailed three-dimensional winds from a mesoscale meteorological model, MM5 (MEDOC). A large number of types of model outputs are being evaluated, including dosages and 15, 30, and 60-minute averaged concentrations. Maximum concentrations on downwind distance arcs are being evaluated as well as concentrations paired in time and space at all samplers. The first set of results concern the maximum 30-minute averaged concentrations, C_{max}, at six downwind distance arcs. It is found that the HPAC configuration using UDM and using the MM5 meteorological inputs (MEDOC) performed better than the others, with a Fractional Bias of 0.06 and a Normalized Mean Square Error (NMSE) of about 3.0. The other options tended to have more overpredictions during the night and underpredictions during the day. The second set of results concerned concentrations paired in space and time and whether the location of the predicted and observed plumes agreed for concentrations above certain thresholds. It is found that, for most sampler locations and times, there was good agreement between the locations of the predicted and observed plumes, but that the predicted plume tended to be broader than the observed plume in most cases.

Corresponding author address: Steven R. Hanna, Hanna Consultants, 7 Crescent Ave., Kennebunkport, ME 04046, hannaconsult@adelphia.net

1. INTRODUCTION

This paper describes the methods and some of the results of an evaluation of the Hazard Assessment and Prediction Capability (HPAC) transport and dispersion modeling system (DTRA 2004, Sykes et al 2007) using the Joint Urban 2003 (JU2003) continuous release tracer data. Allwine et al. (2004) summarize the JU2003 field experiment, which took place in Oklahoma City during July 2003. Clawson et al. (2005) describe the JU2003 SF₆ observations. The ten IOPs had three different source release locations: Botanical Garden (upwind of the downtown area) for IOPs 03 through 07; Westin Hotel (in the built-up downtown area) for IOPs 01, 02, and 08; and Park Avenue (in a street canyon in the downtown area) for IOPs 09 and 10. IOPs 01-06 took place during the day and IOPs 07-10 took place during the night.

The JU2003 tracer concentration and meteorological data are stored in a web-based data archive at Dugway Proving Ground (DPG, 2005). During each of the ten JU2003 IOPs, three continuous releases of SF₆ of 30-minute duration were made at 2-hour intervals, except that only two releases were made during IOP01. Hanna et al. (2007) present the results of a similarity analysis of the JU2003 wind, turbulence, and continuous-release concentration data. Instantaneous (puff) releases of SF₆ also took place during each IOP, but these releases are not discussed or analyzed here (see Zhou and Hanna, 2007, for the results of an analysis of the along-wind diffusion of the puffs). Samplers were set out on a rectilinear grid in the built-up downtown area at distances less than 1 km from the source. Samplers were also set out on three concentric arcs, covering an angular range of about 120° at distances 1, 2, and 4 km to the north of the downtown area (see Figure 1). A close-up view of the downtown (Central Business District) samplers is in Figure 2. The specific sampler locations changed from one IOP to the next, depending on the release location and the wind direction. The averaging time for the samplers was adjustable and was generally set to 5, 15, or 30 minutes. Some of the samplers were always set for 30-minute averages, while others were always set for a shorter period. The analysis in this paper uses 30-minute averaged concentrations, C, normalized by the source emission rate, Q. In the downtown area, where the samplers were on a rectangular grid shown in Figure 2, the authors subjectively assigned each sampler to one of three effective "arc" distances: 0.30, 0.62, and 0.85 km. The data from the sampling arcs at 1, 2, and 4 km were also used.

In addition to the street-level samplers, a few rooftop samplers were employed in the downtown area in order to assess the amount of vertical dispersion that was occurring. However, this paper does not consider the rooftop samplers.

We have found that the first two trials of the daytime IOP05 are more representative of nighttime stable conditions, though the releases took place during the early morning. Figure 4 shows the observed maximum C/Q at each arc distance for four daytime IOPs (3, 4, 5, and 6) for three distances (1, 2, and 4 km) and for releases at 9 am, 11 am, 1 pm, and 3 pm LDT. The relatively high C/Q observations for IOP05 for the 9 and 11 am releases are obvious. The IOP05 trials with relatively high observed C/Q were caused by relatively low mixing depths (less than 200 m). Consequently, IOP05 trials 1 and 2 are removed from some parts of the analysis of the daytime IOPs or are included in the nighttime category. Also, in the evaluations reported here, data from IOPs 01 and 02 are not included because of problems with setting up the input data.

Previous analyses (see Hanna et al., 2007, and Section 2) of the JU2003 observed 30-minute averaged maximum concentrations on several downwind distance arcs showed that values of C/Q were generally about three times higher during the night IOPs than during the day IOPs. We hypothesized that this relatively small difference is due to the relatively small differences in near-ground urban stability, ranging from slightly unstable during the day to slightly stable during the night.

This paper considers two urban HPAC options (Urban Dispersion Model (UDM) and Urban Canopy (UC)). The paper also considers four meteorological input options:

BDF - Basic National Weather Service (NWS) default

MED - Mesoscale Meteorological Model-Version 5 (MM5) MEDOC outputs

AVG - Average wind speed and direction from all anemometers (Hanna et al., 2007)

UPWIND - Wind speed and direction from DPG Portable Weather Instrumentation Data System (PWIDS) #15 on the Post Office, located just upwind of the downtown area, with observed mixing heights based on the upwind Pacific Northwest National Laboratory (PNNL) radiosonde data.

The AVG wind inputs are based on the speeds and directions listed in the last two columns of Table 1

2. OBSERVED VARIATION OF CONCENTRATION WITH STABILITY

The analysis in this section focuses on the maximum 30-minute averaged concentration, C_{max} , observed for a given release by the set of samplers on a given distance arc. More details are given in Hanna et al. (2007). Hanna et al. (2003), Venkatram et al. (2004), Britter

(2005), and Neophytou and Britter (2004) have suggested the following dimensionless similarity relation for continuous releases near street level in downtown areas with many tall buildings covering an area of 1 km^2 or larger:

$$C_{max}uH^2/Q = F(x/H)$$

where F indicates a generalized function, u is the spatially-averaged wind speed in the downtown urban canopy, H is the average building height, Q is the continuous mass emission rate, and x is downwind distance. Neophytou and Britter (2004) and Britter (2005) suggest that $F(x/H)$ equals about $A(x/H)^2$ for $x/H < \text{about } 50$, where A is a "constant" of order 10. The H cancels out and it follows that $C_{max}u/Q = A x^{-2}$.

As shown in Figure 4, we have found that the first two trials of IOP05 are more representative of the night, though, since they occur during the early morning and the mixing depths are observed to be relatively low (less than 200 m) due to the presence of thunderstorms in the area. Thus IOP05 trials 1 and 2 are included in the nighttime category in the plots discussed below.

In Figure 5a, for daytime conditions, the JU2003 $C_{max}u/Q$ data for individual trials are seen to agree well with the trend with distance, x , of the averaged DAPPLE data. The x^{-2} relation appears to be approximately followed out to distances of 4 km during the daytime. However, the "constant" A in the x^{-2} relation is closer to 3 than to 10. The scatter of the data from the individual JU2003 trials about the best fit line is approximately \pm a factor of three (including about 90 % of the points).

In Figure 5b, for nighttime conditions, the SLC Urban 2000 averaged $C_{max}u/Q$ data are quite close to the median of the JU2003 data. There are 14 nighttime trials during JU2003. The JU2003 points on the 0.2 km arc are slightly lower in magnitude than those on the 0.38 km arc. The reason for the lower C_{max} values on the closer arc may be that there are fewer samplers on the 0.2 km arc, thus allowing the tracer cloud to sometimes not have its C_{max} captured. The points on Figure 5b tend to verify the $C_{max}u/Q = A x^{-2}$ relation, with A equal to about 10, for distances less than and equal to 1 km. The data tend to be above the $10 x^{-2}$ line by about a factor of two at $x = 2$ km and a factor of four at $x = 4$ km. The discrepancy is likely due to the inhibited vertical mixing at night as the cloud passes into the residential areas.

As seen in Figures 5a and 5b, the observed concentration data can be fit by $C_{max}u/Q = 3 x^{-2}$ during the daytime and by $C_{max}u/Q = 10 x^{-2}$ during the nighttime. Thus there is a factor of about three difference between daytime and nighttime $C_{max}u/Q$, despite the fact that the street-level turbulence observations indicated little day-night difference and similar slightly-unstable values of σ_T/T and L . The reason for the day-night difference in $C_{max}u/Q$ is probably due to the fact that there are stable conditions aloft over the built-up Oklahoma City urban area at night (Lundquist and Mirocha, 2006). Note that the $C_{max}u/Q$ data from other cities (London DAPPLE and Salt Lake City Urban2000) plotted on Figures 5a and 5b confirm

this day-night difference of about a factor of three. We stress that these results are for near-surface continuous releases of non-buoyant tracers.

3. HPAC OPTIONS AND INPUTS

HPAC was used to calculate SF₆ tracer concentrations at the locations of the bag samplers within the central business district (CBD) and the three outer arcs (at 1, 2, and 4 km). As discussed in section 1, the model runs used two HPAC urban model configurations and four different sets of meteorological data. Model source parameters included the initial Gaussian spread σ_y and σ_z (set to 0.232 m), the tracer release duration (30 minutes), the release height (1.9 m), and the mass dissemination rate, Q (obtained from the JU2003 database). Cloud cover was set based on the standard hourly NWS observations. Surface moisture was set to “normal” and gridded terrain elevation was used except for the HPAC model runs that used the MM5 gridded data (the MED meteorological option), which already contained the terrain information. With two exceptions, boundary layer calculations were set to default. The gridded MM5 MEDOC output files include the mesoscale model’s boundary surface heat flux and boundary layer depth estimates. In the case of the UPWIND meteorological option, the boundary layer depth was estimated by the authors from PNNL radiosonde soundings for each continuous release. (Reasonable agreement was found between boundary layer depths inferred from the PNNL and Argonne National Laboratory radiosonde soundings and those estimated from DPG’s FM/CW radar.) The PNNL radiosonde data set was selected because of the close proximity of the balloon release site to PWIDS #15 and its location upwind of the CBD. Default values were used for other HPAC inputs such as the Bowen ratio (2) albedo (0.16), canopy height (30 m, the value used for the Urban 2000 study), and canopy flow index (2). All HPAC runs except those using the MED meteorological option used HPAC’s SWIFT diagnostic wind field model to derive mass-consistent wind fields. The SWIFT default parameters were used in these runs with the exception of the wind field update interval, which was set to 1 hour for the BDF and AVG meteorological options, and to 10 minutes for the UPWIND meteorological option. Other HPAC input parameters were: i) Conditional averaging time set to 30 minutes for comparison with 30-minute average concentrations; ii) No large scale variability; and iii) Sampling height set to 1.5 m (the height of the bag samplers).

4. MODEL EVALUATION METHODS

The BOOT statistical model evaluation software (Chang and Hanna, 2004) was used to compare predicted and observed arc maximum 30-minute averaged C/Q paired and unpaired in space and time. The limited results presented in Section 5 focus on the maximum C/Q on a given downwind arc. The following performance measures were used, where we let $X=C/Q$:

$$\text{Fractional Bias } FB = 2\langle X_o - X_p \rangle / (\langle X_o \rangle + \langle X_p \rangle)$$

$$\text{Normalized Mean Square Error } NMSE = \langle (X_o - X_p)^2 \rangle / (\langle X_o \rangle + \langle X_p \rangle)$$

$$\text{Fraction of } X_p \text{ within a factor of two of } X_o \text{ (FAC2)}$$

$$\text{Geometric Mean } MG = \exp(\langle \ln X_o \rangle - \langle \ln X_p \rangle)$$

$$\text{Geometric Variance } VG = \exp(\langle (\ln X_o - \ln X_p)^2 \rangle)$$

Subscripts p and o refer to predicted and observed, and the symbol $\langle \rangle$ represents an average. Residual plots were also used in the evaluation, where the ratio of X_p/X_o was plotted versus downwind distance, x. The five lines on the box plot represent the 98th, 84th, 50th, 16nd, and 2th percentiles, respectively, for the group of data considered.

In addition to the above comparisons of maximum concentrations on an arc, paired-in-space-and-time comparisons were made using all sampler data. The comparisons consider two threshold values, 25 and 250 ppt, consistent with the Warner et al. (2007) study. In these comparisons, observations are not allowed to drop below the SF₆ background concentration (5 ppt) and the background is added to all model predictions. A quantitative estimate of model performance for data paired in time and space is two-dimensional measure of effectiveness (MOE) defined by Warner et al. (2007):

$$MOE = (MOE_{FN}, MOE_{FP}) = \left(\frac{A_p \cap A_o}{A_p \cap A_o + A_{FN}}, \frac{A_p \cap A_o}{A_p \cap A_o + A_{FP}} \right)$$

where $A_p \cap A_o$ means the number of samplers where both observations and model predictions are above the threshold, A_{FN} means the number of samplers where observations are above but predictions are below the threshold (false-negative), and A_{FP} means the number of samplers where observations are below but predictions are above the threshold (false-positive). In other words, all that matters is whether observations and predictions are above or below the threshold. The degree to which observations and predictions are above or below the threshold does not matter.

In order to better understand these paired-in-time-and-space results, the samplers with observations and/or predictions exceeding the threshold of 25 ppt from all IOPs and for the three continuous SF₆ release trials in each IOP are plotted. The dots in the plots are colored green, red, or blue, according to the following convention:

“Green” samplers: both observations and predictions are above 25 ppt (overlap)

“Red” samplers: observations above and predictions below 25 ppt (false negative)

“Blue” samplers: observations below and predictions above 25 ppt (false positive)

5. RESULTS FOR ARC MAXIMUM C COMPARISONS

The BOOT software was used to calculate the performance measures and generate the residual plots as defined above for the arc maximum concentrations for the eight model configurations (two urban model options and four alternate meteorological inputs). Table 2 presents the performance measures for the four Met options and the two urban model options, calculated separately for the day and night IOPs. Figure 6 shows the residual plots for urban options UDM and UC coupled with the MED meteorological option. It was necessary to split the analysis into day and night because the first comparisons showed that most of the eight model configurations had a tendency to overpredict at night and underpredict during the day. Warner et al. (2007) found similar biases in their evaluations of HPAC with the JU2003 data for a wider variety of urban model options and meteorological inputs. In our study, IOP05 was removed from the daytime statistics because, as described in Section 2, it was associated with an anomalous stable boundary layer with low mixing depths in the morning due to outflows from nearby large thunderstorms. The removal of IOP05 reduces NMSE and VG but does not change the overall conclusions about model performance. The MM5 MEDOC inputs were better able to account for the low mixing depths than the other meteorological options.

Figures 7 through 10 present the residual plots for all options. Figures 7 and 8 are for the day IOPs and Figures 9 and 10 are for the night IOPs. In each figure, the panels to the left are for UDM and the panels to the right are for UC. Figures 7 and 9 have the BDF met option on the top and MED on the bottom, and Figures 8 and 10 have the AVG met option on the top and UPWND on the bottom.

Some basic conclusions from the performance measures in Table 2 and residual plots in Figures 6 – 10 are:

- For most model and meteorological input combinations, there is a tendency to overpredict by an approximate factor of 3 or 4 at night and underpredict by an approximate factor of 2 during the day.
- For the daytime IOPs (03, 04, and 06), MED-UC and UPWND-UDM tend to have the least bias, lowest scatter and highest FAC2; and little trend with x . MED-UDM has an underprediction tendency of about a factor of 3 or 4 at small x . UDM and UC simulations of C/Q tend to agree for all meteorological options at $x > 1$ km (outside of the built-up area). For all meteorological options, the ratio of the concentrations predicted by UC to UDM is about 3 or 4 at small x (inside of the built-up area). UDM simulations are always lower than

the observed values (by factor of 2 to 5) at small x for all meteorological options.

- For the nighttime IOPs (07, 08, 09, and 10), MED-UDM has the least bias, lowest scatter, and highest FAC2; and has little trend of the residuals with x . Unlike the daytime runs, UDM and UC simulations do not agree as well at large x . The same bias occurs at all x . For all meteorological options, the ratio of the concentrations predicted by UC to UDM is about 2 at all x . The AVG and UPWND meteorological options lead to large mean overpredictions of a factor of 3 to 10.
- In general, most model options yield a much larger day-night difference in C/Q than the factor of three or four difference suggested by the observations summarized in Section 2.

Our HPAC evaluations to date and the evaluations reported by other groups (e.g., Warner et al., 2007) agree that urban HPAC overpredicts during the night and underpredicts (by a smaller amount) during the day. The observed day-night difference is about three or four, but the HPAC-simulated difference is much larger for most options. The difference is larger than three or four even for the better performing Met option – MED. This type of behavior suggests that the model may be using too broad of a diurnal range in stabilities. The analyses by Hanna et al. (2007) of sonic anemometer data (including calculations of surface heat fluxes and Monin Obukhov lengths L) suggest that the stability in the built-up downtown area of OKC is near neutral, and usually slightly unstable, throughout the diurnal cycle. This result can be attributed to the strong mechanical mixing due to the buildings and anthropogenic heat input. At night, the slightly-unstable near-surface urban boundary layer is capped at a height of about 200 m by a more stable layer representative of the upwind boundary layer. It is hypothesized that urban HPAC would do better if it used a more nearly-neutral stability parameterization throughout the diurnal cycle, which would ameliorate the nighttime overpredictions and daytime underpredictions. Currently, the HPAC meteorological preprocessor assumes that the sensible heat flux in the upwind area is also valid in the urban area. (When used with MM5 inputs, HPAC uses the heat fluxes computed by the mesoscale model.) Use of the upwind sensible heat flux in the urban area is probably reasonable during the day, but is not valid at night, which may explain the larger biases at night. Note that the HPAC meteorological preprocessor does modify the friction velocity u_* based on the increased roughness in the urban area.

As stated earlier, the observed arc-maximum 30-minute average normalized concentration data from JU2003 indicate that, on average in the CBD ($x < 1$ km), the daytime C/Q's are about a factor of 3 smaller than the nighttime C/Q's. At $1 \text{ km} < x < 4 \text{ km}$, the day-night difference in C/Q increases to about a factor of 8, due to the increasing nighttime stability in the suburbs as the

plume travels out of the CBD. The factor of 3 difference in CBD C/Q is consistent with an assumption of slightly unstable conditions during the day and very slightly-stable conditions during the night in the CBD. If a dispersion model is going to do well with these data, it must be able to simulate the observed factor of 3 day-night difference in C/Q. But because most HPAC model options showed large overpredictions during the night and large underpredictions during the day, it is concluded that those options are overstating the day-night difference in near-ground urban stability.

We hesitate to overinterpret these results. Just because a model combination seems to do better than another, it could be because that model tends to over or underpredict with respect to the other models and may have a compensating error. Until additional analyses are carried out, such as investigation of the effective wind speeds being used by each meteorological input option, it is difficult to untangle the possible effects of different meteorological inputs and decide which is more realistic. For example, it could be that the model that is currently performing better is using an effective wind speed that is too low or too high (i.e., there are compensating errors).

6. RESULTS FOR PAIRED-IN-SPACE-AND-TIME COMPARISONS

This section contains the results of the paired-in-space-and-time comparisons. All sampler data are used here, in contrast to the comparisons in Section 5, where only the maximum concentration on each distance arc was used. The methodology is described in Section 4.

The Measure of Effectiveness (MOE) results are presented separately for daytime and nighttime IOPs in Table 3, where IOP05 is excluded from daytime IOPs in the first daytime table. A perfect model performance is indicated by $MOE = (1, 1)$. The performance measures listed in Table 3 can be shown in a standard plot of MOE_{FN} versus MOE_{FP} , with Figure 11 containing an example for the daytime IOPs and a threshold of 25 ppt. This figure is seen to be not too informative, however, because the points are clustered close together and do not seem to be related well to the performance measures for C_{mx} in Table 2.

The samplers with observations and/or predictions exceeding the threshold of 25 ppt for all IOPs and for the three continuous SF_6 release trials in each IOP are indicated by colored dots in Figures 12 through 19. The first two 30-min periods for each release are plotted for each IOP. The figures show significant samplers based on an SF_6 threshold of 25 ppt and HPAC predictions given by the UPWIND met option and UDM model option, which provided fairly good agreement for most trials.

It is seen that there are many more green dots than either red or blue dots, indicating that most samplers that are "hit" by the observed plume are also "hit" by the predicted plume. This helps to provide confidence for decision makers (such as emergency managers) who must use the model results in order to decide who to

evacuate and/or where to send emergency responders. However, because of the nature of the field experiment design, these data trials (IOPs) are likely to show better agreement than randomly selected time periods, since the field experiments were carried out only if the winds were strong enough and persistent enough that the experimentalists were confident that the sampler network would capture the plume.

Figures 12-19 also show that there are more blue dots than red dots, indicating more periods when the predicted plume is present but not observed (i.e., false positive) than when the observed plume is present but not predicted (i.e., false negative). From the point of view of protecting the public, a false positive is better than a false negative. The number of blue dots is larger for the daytime IOPs (3-6) than for the nighttime IOPs (7-10), and the reason is that the model is simulating the plume to be too broad during the day, which also tends to lead to underprediction of the centerline maximum concentration seen in Table 2.

In all of the plots for the nighttime IOPs, there are red dots at the farthest (4 km) arc for the first thirty minute period, suggesting that the predicted plume is not moving as fast as the observed plume. Also, for the nighttime IOPs, the plume width continues to be overpredicted (blue dots) in the downtown area at $x < 1$ km, but the predicted and observed plume widths tend to match at $x > 1$ km.

There are no cases in Figures 12 -19 where the predicted plume completely missed the observed plume. This result is probably pre-ordained by the use of the observed winds just upwind of the downtown area, thus assuring accurate plume directions.

ACKNOWLEDGEMENTS

This research has been sponsored by the National Science Foundation, the Department of Homeland Security, and the Defense Threat Reduction Agency.

REFERENCES

Allwine K. J., M. Leach, L. Stockham, J. Shinn, R. Hosker, J. Bowers and J. Pace, 2004, Overview of Joint Urban 2003 – An atmospheric dispersion study in Oklahoma City'. Preprints, Symposium on Planning, Nowcasting and Forecasting in the Urban Zone. American Meteorological Society, January 11-15, 2004, Seattle, Washington.

Britter, R.E., 2005: DAPPLE: Dispersion of Air Pollutants and their Penetration into the Local Environment. <http://www.dapple.org.uk>

Britter, R.E. and S.R. Hanna, 2003: Flow and dispersion in urban areas. *Annu. Rev. Fluid Mech.*, **35**, 469-496.

Chang, J.C., and S.R. Hanna, 2004: Air quality model performance evaluation. *Meteorol. and Atmos. Phys.*, **87**, 167-196.

Clawson, K., R. Carter, D. Lacroix, C. Biltoft, N. Hukari, R. Johnson, J. Rich, S. Beard and T. Strong, 2005, Joint Urban 2003 (JU2003) SF₆ Atmospheric Tracer Field Tests, NOAA Tech Memo OAR ARL-254, Air Resources Lab., Silver Spring, MD, 162 pages + Appendices.

DTRA, 2004: HPAC Version 4.04.011 (DVD containing model and accompanying data and document files). Available from DTRA, 6801 Telegraph Rd., Alexandria, VA.

Dugway Proving Ground, 2005: Data Archive for JU2003. <https://ju2003-dpg.dpg.army.mil>

Hanna, S.R., R. Britter, and P. Franzese, 2003: A baseline urban dispersion model evaluated with Salt Lake City and Los Angeles tracer data. *Atmos. Environ.*, **37**, 5069-5082.

Hanna, S., J. White and Y. Zhou, 2007, Observed winds, turbulence, and dispersion in built-up downtown areas of Oklahoma City and Manhattan. *Bound.- Lay. Meteorol.* (in press).

Neophytou, M.K. and R.E. Britter, 2004: A simple correlation for pollution dispersion prediction in urban areas. DAPPLE Cambridge Note 1, January 2004, <http://www.dapple.org.uk>

Venkatram, A., V. Isakov, D. Pankratz, J. Heumann and J. Yuan, 2004: The analysis of data from an urban dispersion experiment. *Atmos. Environ.* **38**, 3647-3659.

Sykes, R.I., S. Parker, D. Henn and B. Chowdhury, 2007, SCIPUFF Version 2.3 Technical Documentation. L-3 Titan Corp, POB 2229, Princeton, NJ 08543-2229, 336 pages.

Warner, S., N. Platt, J. Urban and J. Heagy, 2007: Comparisons of transport and dispersion model predictions of the JU2003 field experiment. *J. Applied Meteorol. and Climatol.*, in press.

Zhou, Y. and S. Hanna, 2007, Along-wind dispersion of puffs released in a built-up urban area. *Bound.-Lay. Meteorol.* (in press)

Table 1. Summary of observed wind speed (WS) and wind direction (WD) during JU2003. Winds are averaged over each 8-hour duration IOP. Winds are also averaged within seven groups of similar types of anemometer locations. Overall averages are given in the right two columns and in the bottom row.

	Exposed bldg top downtown 7 sites dpg & pnnl z = 14 to 153 m		Sheltered Bldg tops in dense downtown area 14 lanl and 9 uou sites z = 19 to 47 m		Semiexposed downtown in bldgs but not street level 5 dpg sites z > 10 m		Street canyon downtown all z = 8 m 18 dpg and 2 OU sites		Semi-exposed park or resid. 7 dpg, 1 lnl crane 2 arl towers, all 8-10 m		Suburban/rural upwind/downwind		Airport		Average over all groups	
	Wind group 1a		Wind group 1b		Wind group 2		Wind group 3		Wind group 4		Wind group 5		Wind group 6		Avg WS	Avg WD
	WS m/s	WD	WS m/s	WD	WS m/s	WD	WS m/s	WD	WS m/s	WD	WS m/s	WD	WS m/s	WD	m/s	
Avg IOP01	3.4	167	0.78	207	1.5	150	1.1	155	1.5	138	2.7	193	1.8	35	1.8	149
Avg IOP02	4.3	215	0.77	275	2.6	191	1.4	222	1.8	221	3.5	214	5.0	177	2.8	216
Avg IOP03	6.4	196	0.58	232	3.6	178	1.9	205	2.7	182	5.4	201	5.7	177	3.7	196
Avg IOP04	6.1	203	0.77	235	3.9	184	2.1	212	2.8	184	5.3	204	6.8	171	4.0	199
Avg IOP05	3.8	192	0.74	222	1.8	172	1.2	189	1.6	194	3.2	193	7.5	174	2.8	191
Avg IOP06	4.3	195	0.44	202	2.6	180	1.4	198	2.2	176	3.7	196	7.1	209	3.1	194
Avg IOP07	4.8	207	0.82	270	2.5	189	1.6	211	1.5	213	2.9	197	3.3	230	2.5	217
Avg IOP08	6.1	143	0.93	170	2.8	147	1.7	152	2.9	157	4.3	165	8.1	167	3.8	157
Avg IOP09	5.5	182	0.49	153	2.8	153	1.4	199	2.3	168	3.3	186	6.2	198	3.2	177
Avg IOP10	5.0	193	0.67	227	2.7	173	1.5	209	1.9	184	2.5	192	2.6	223	2.4	200
Avg All	5.0	189	0.70	219	2.7	172	1.5	195	2.1	192	3.7	194	5.4	176	3.0	191

Table 2. Performance measures for evaluations of HPAC with the JU2003 data, emphasizing the arc maximum C_{max}/Q . See text for definitions of performance measures, meteorological options, and model options. Note that when $FB = -2/3$, there is a mean factor of two overprediction, and when $FB = +2/3$, there is a mean factor of two underprediction. $FB = 0$ and $MG = 1$ indicate an unbiased model.

IOP03, IOP04, & IOP06 (daytime only, excluding IOP05)

Met Options	Model Options	FB	NMSE	FAC2	MG	VG
BDF	UDM	0.88	3.4	19%	2.28	3
BDF	UC	-0.29	1.6	59%	1.41	2
MED	UDM	0.91	3.9	50%	1.81	2.1
MED	UC	-0.38	1.9	70%	0.89	1.6
AVG	UDM	1.02	4.9	46%	2.15	2.4
AVG	UC	0.52	1.4	63%	1.59	1.6
UPWND	UDM	0.44	1.2	74%	1.04	1.5
UPWND	UC	-0.89	3.9	44%	0.47	2.3

IOP07-IOP10 (nighttime only)

Met Options	Model Options	FB	NMSE	FAC2	MG	VG
BDF	UDM	-1.15	20.1	32%	1.58	1.3E+07
BDF	UC	-1.56	34.0	5%	1.45	1.3E+10
MED	UDM	-0.47	7.2	49%	1.02	3.4
MED	UC	-1.19	13.0	25%	0.36	22.6
AVG	UDM	-1.35	31.0	28%	0.32	9.8
AVG	UC	-1.74	85.2	3%	0.11	385.0
UPWND	UDM	-1.30	22.8	29%	0.38	6.9
UPWND	UC	-1.62	38.0	5%	0.17	116.0

Table 3 Measure of Effectiveness (MOE) performance measures for evaluations of HPAC with the JU2003 data, paired in time and space. See text for definitions of MOE, meteorological options, and model options. Note that FN refers to false negatives and FP refers to false positives. MOEs are listed for SF₆ concentration thresholds of 25 and 250 ppt. Figure 11 is an example of a MOE plot. Figures 12-19 show the samplers that agree, that have FPs and that have FNs for the IOPs being studied, and from which the MOEs were calculated.

		25 ppt		250 ppt	
IOP03, IOP04, & IOP06 (day only, excluding IOP05)					
Met Options	Model Options	MOE _{FN}	MOE _{FP}	MOE _{FN}	MOE _{FP}
BDF	UDM	0.82	0.61	0.49	0.65
BDF	UC	0.75	0.58	0.48	0.61
MED	UDM	0.79	0.61	0.44	0.65
MED	UC	0.72	0.61	0.44	0.64
AVG	UDM	0.89	0.58	0.51	0.63
AVG	UC	0.86	0.60	0.53	0.66
UPWND	UDM	0.95	0.66	0.73	0.69
UPWND	UC	0.83	0.67	0.73	0.62

		25 ppt		250 ppt	
IOP07-IOP10 (night only)					
Met Options	Model Options	MOE _{FN}	MOE _{FP}	MOE _{FN}	MOE _{FP}
BDF	UDM	0.68	0.49	0.62	0.45
BDF	UC	0.29	0.54	0.24	0.41
MED	UDM	0.67	0.62	0.50	0.55
MED	UC	0.43	0.67	0.37	0.57
AVG	UDM	0.86	0.41	0.82	0.42
AVG	UC	0.67	0.63	0.61	0.50
UPWND	UDM	0.93	0.55	0.92	0.58
UPWND	UC	0.68	0.78	0.62	0.65

		25 ppt		250 ppt	
IOP03-IOP06 (day only)					
Met Options	Model Options	MOE _{FN}	MOE _{FP}	MOE _{FN}	MOE _{FP}
BDF	UDM	0.71	0.56	0.40	0.59
BDF	UC	0.64	0.54	0.38	0.57
MED	UDM	0.74	0.59	0.41	0.58
MED	UC	0.69	0.59	0.41	0.58
AVG	UDM	0.88	0.60	0.47	0.65
AVG	UC	0.85	0.62	0.49	0.68
UPWND	UDM	0.93	0.64	0.77	0.65
UPWND	UC	0.83	0.65	0.72	0.57

IOP 04 Sampling Arcs

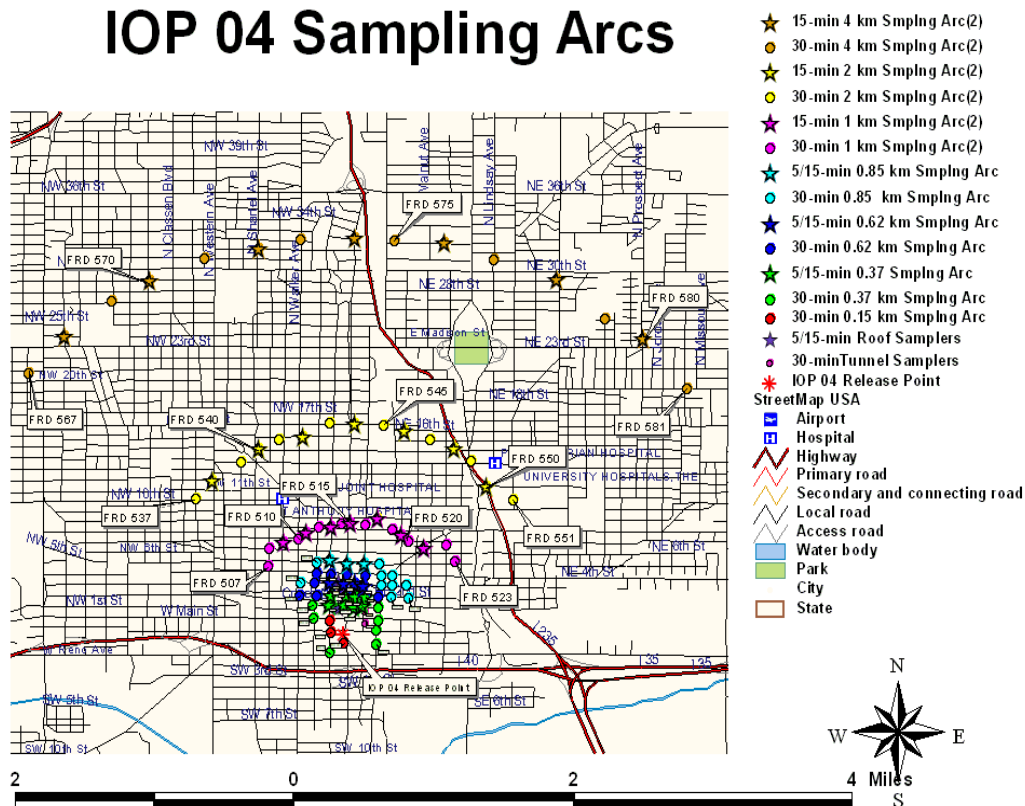


Figure prepared by John White of DPG

Figure 1. Map of Oklahoma City, site of Joint Urban 2003 (JU2003) field experiment. Locations of NOAA Air Resources Laboratory Field Research Division (ARLFRD) SF₆ samplers are shown, as used in IOP04. Data from these samplers were analyzed to generate the summary results for continuous releases in this paper.

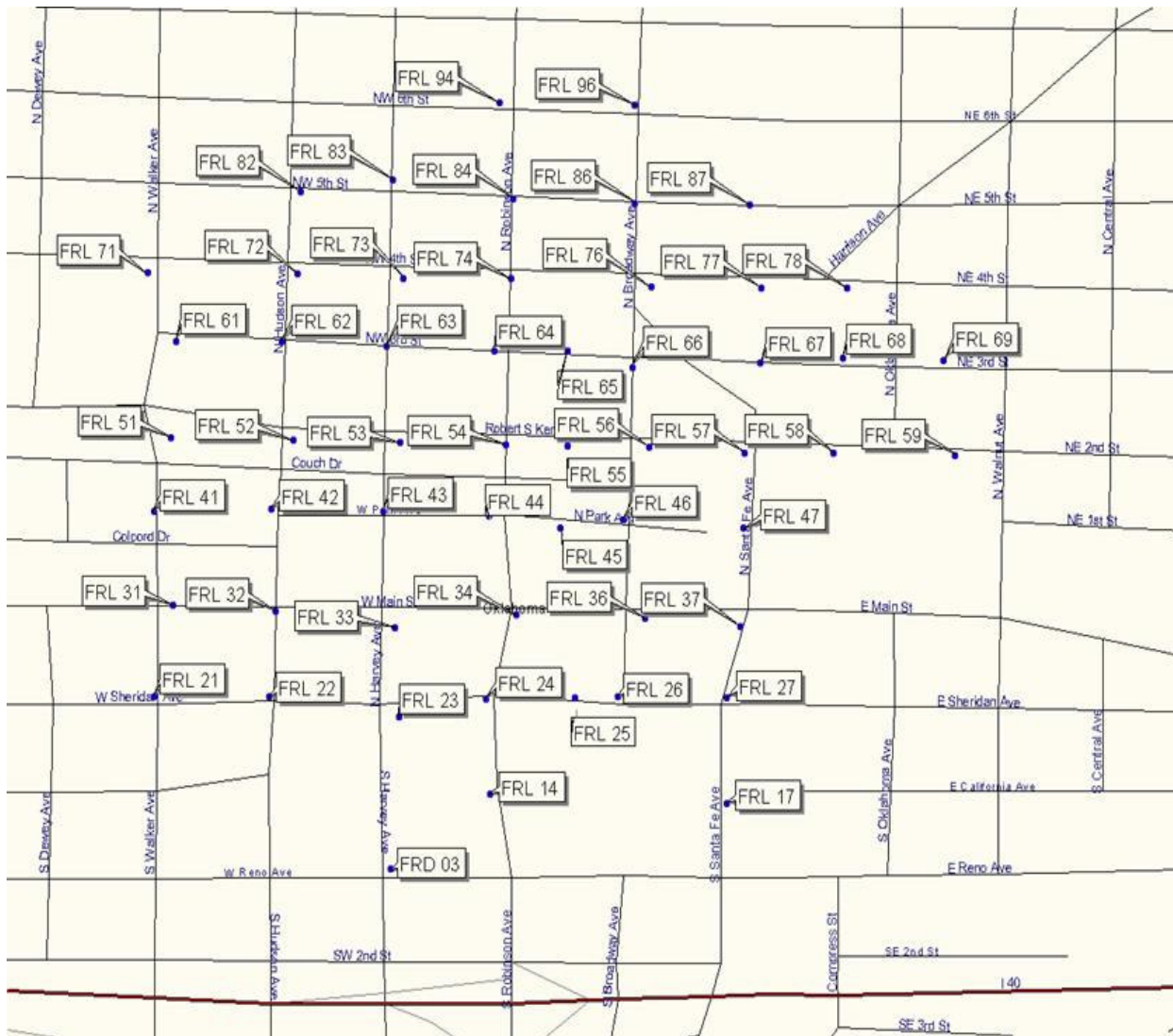


Figure 2. JU2003 SF₆ samplers in the Central Business District of Oklahoma City. This is the inner part of Figure 1.

Model Domain

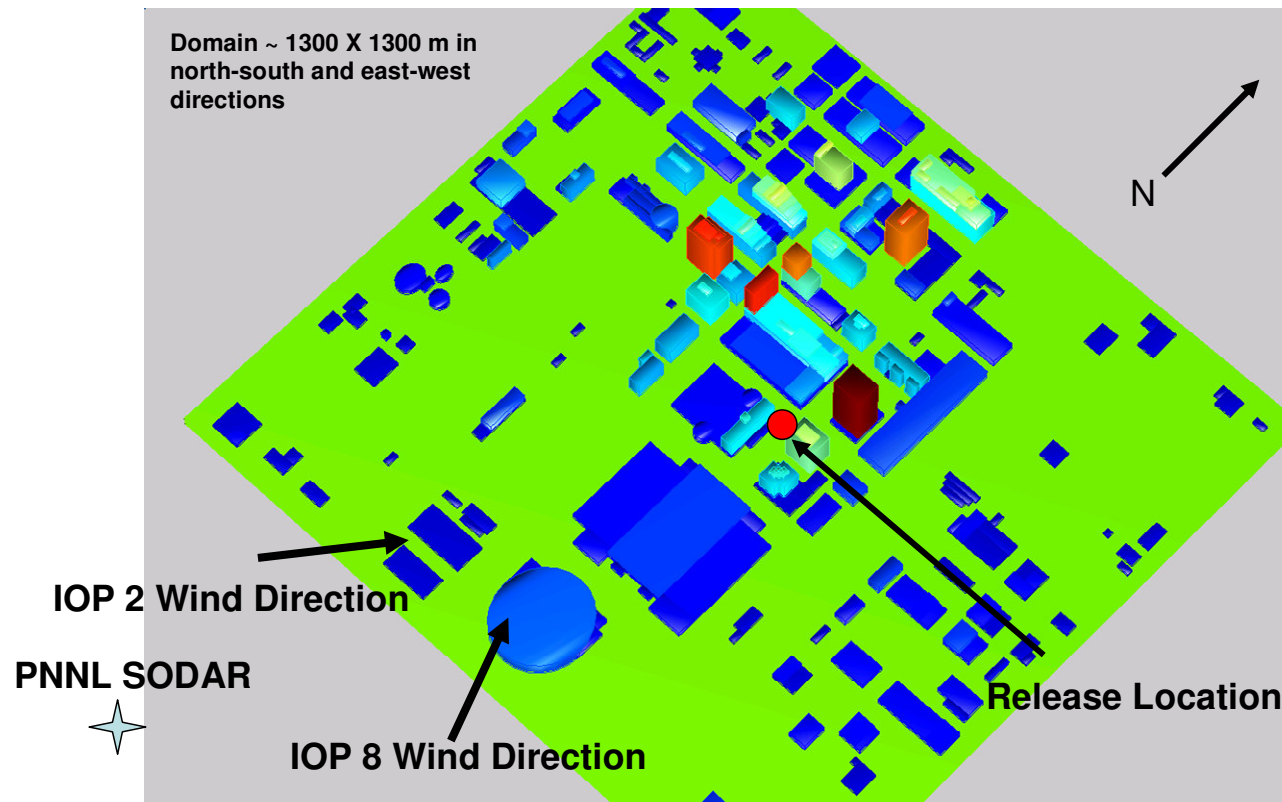


Figure 3. 3-D view of buildings in Central Business District of Oklahoma City. The release location is for the “Westin” releases. Figure provided by Michael Brown.

Comparison of Daytime Arc Max Concentrations over the Three Outer Arcs

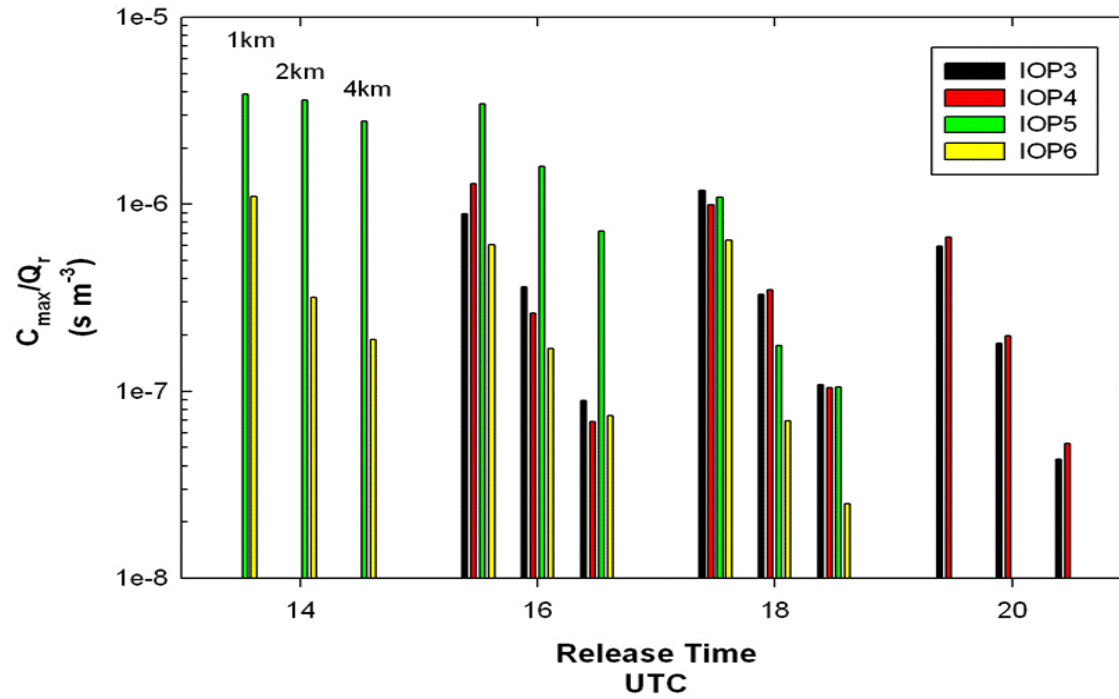


Figure 4. Maximum 30-min average normalized observed arc maximum concentration, C_{\max}/Q_r , on the 1, 2, and 4 km sampling arcs for the four daytime IOPs for release times of 14, 16, 18 and 20 UTC (i.e, 9, 11, 13, and 15 LDT, respectively). The intent of this figure is to demonstrate the exceptionally large observed C_{\max}/Q_r values for IOP05 for the 9 and 11 am LDT release times.

Observed Cu/Q for OKC day trials versus x

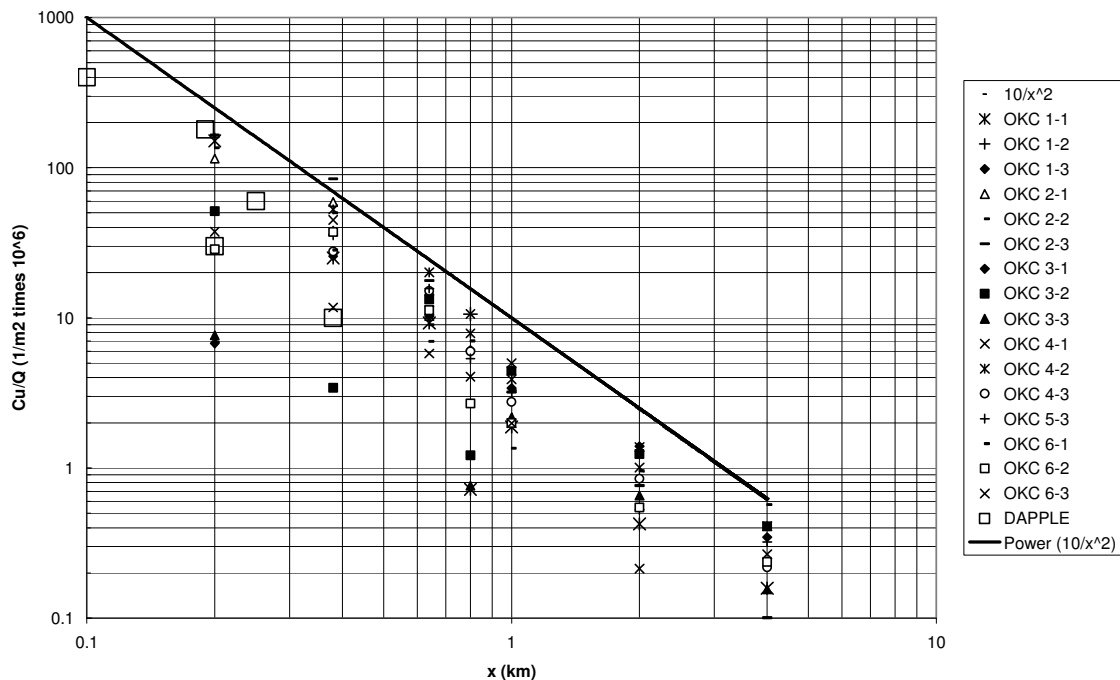


Figure 5a. Summary plot of observed Cu/Q versus x for daytime trials during JU2003 and observed averaged for DAPPLE. C is the maximum 30-minute averaged concentration observed along a cross-wind arc of monitors at a given downwind distance, x . The line given by $Cu/Q = 10/x^2$ is drawn, which Neophytou and Britter (2004) and others have suggested as valid for $x/H < 50$, or for $x < 1$ km when mean building height, H , is 20 m.

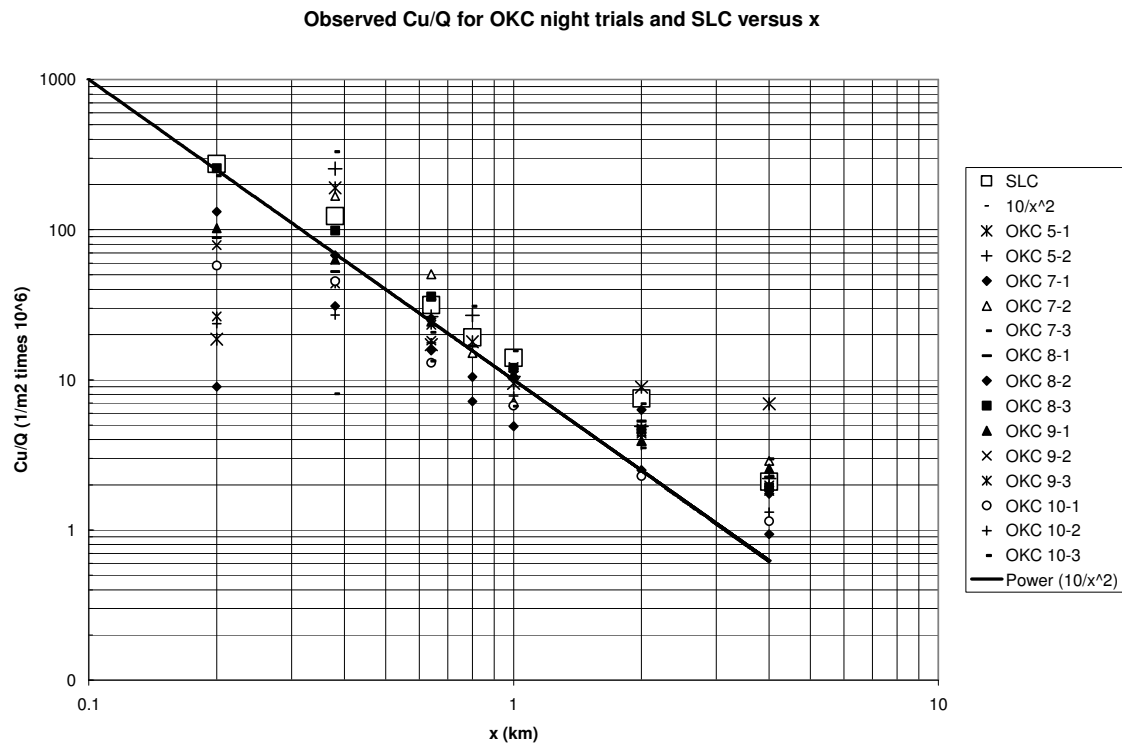


Figure 5b. Summary plot of observed Cu/Q versus x for nighttime trials during JU2003 and observed averaged values for Urban 2000. C is the maximum 30-minute averaged concentration observed along a cross-wind arc of monitors at a given downwind distance, x . The line given by $Cu/Q = 10/x^2$ is drawn, which Neophytou and Britter (2004) and others have suggested as valid for $x/H < 50$, or for $x < 1$ km when mean building height, H , is 20 m.

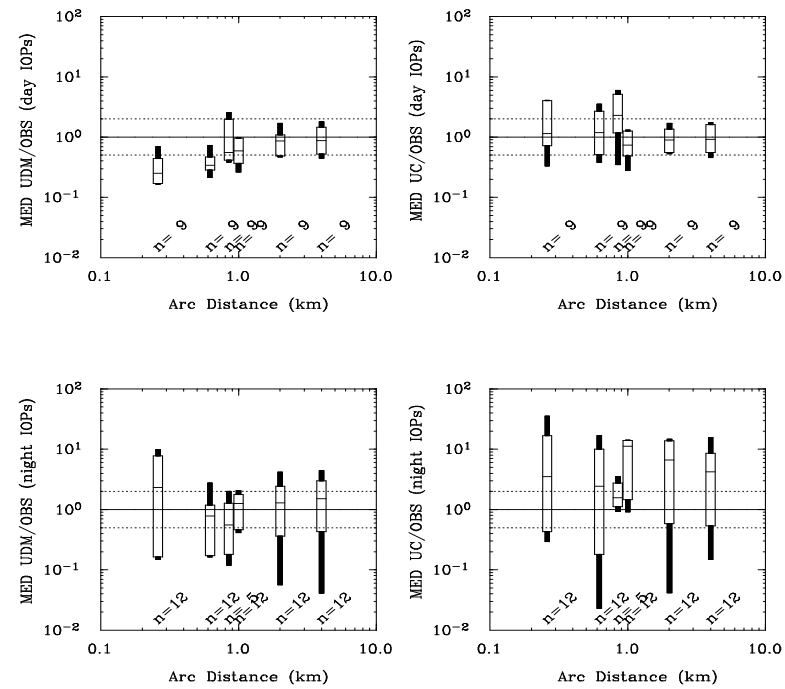


Figure 6. Residual plots (X_p/X_o vs x) of arc max concentrations, C_{max} , for HPAC urban options UDM and UC with MM5 MEDOC meteorological inputs, for day (top) and night (bottom) IOPs. The significant lines on the box plots indicate, from bottom to top, the 2th, 16nd, 50th (i.e., the median), 84th, and 98th percentiles of the n X_p/X_o points at that arc distance.

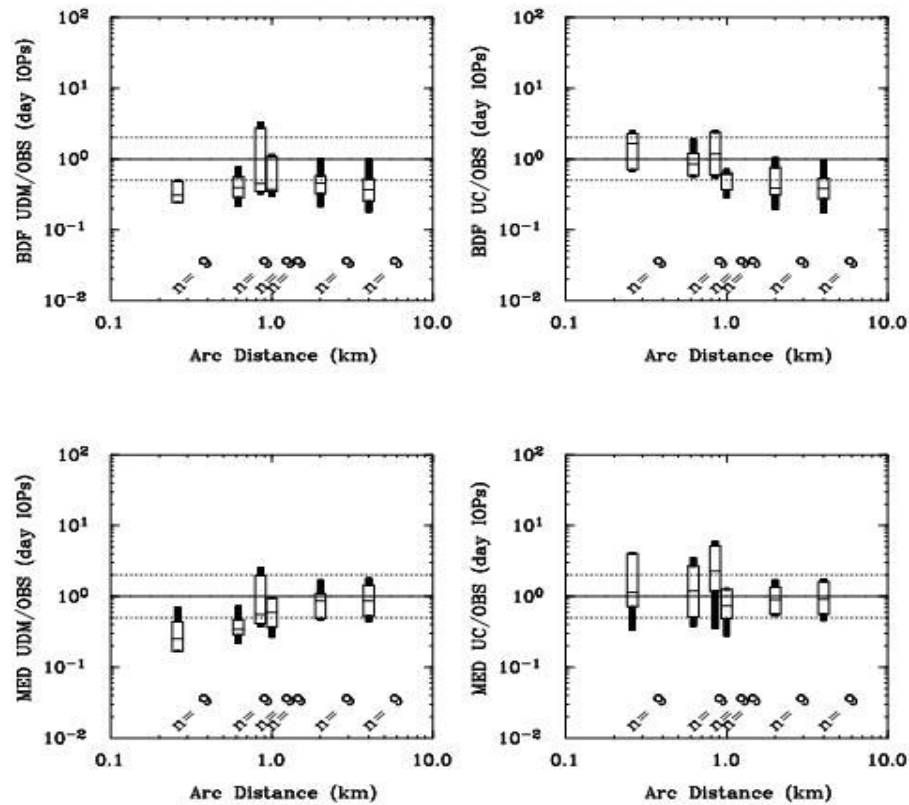


Figure 7. Residual plots (X_p/X_o vs x) of arc max concentrations, C_{max} , for HPAC urban options UDM and UC with Basic Default (BDF) (top) and MM5 MEDOC (bottom) meteorological inputs, for day IOPs. The significant lines on the box plots indicate, from bottom to top, the 2th, 16th, 50th (i.e., the median), 84th, and 98th percentiles of the n X_p/X_o points at that arc distance.

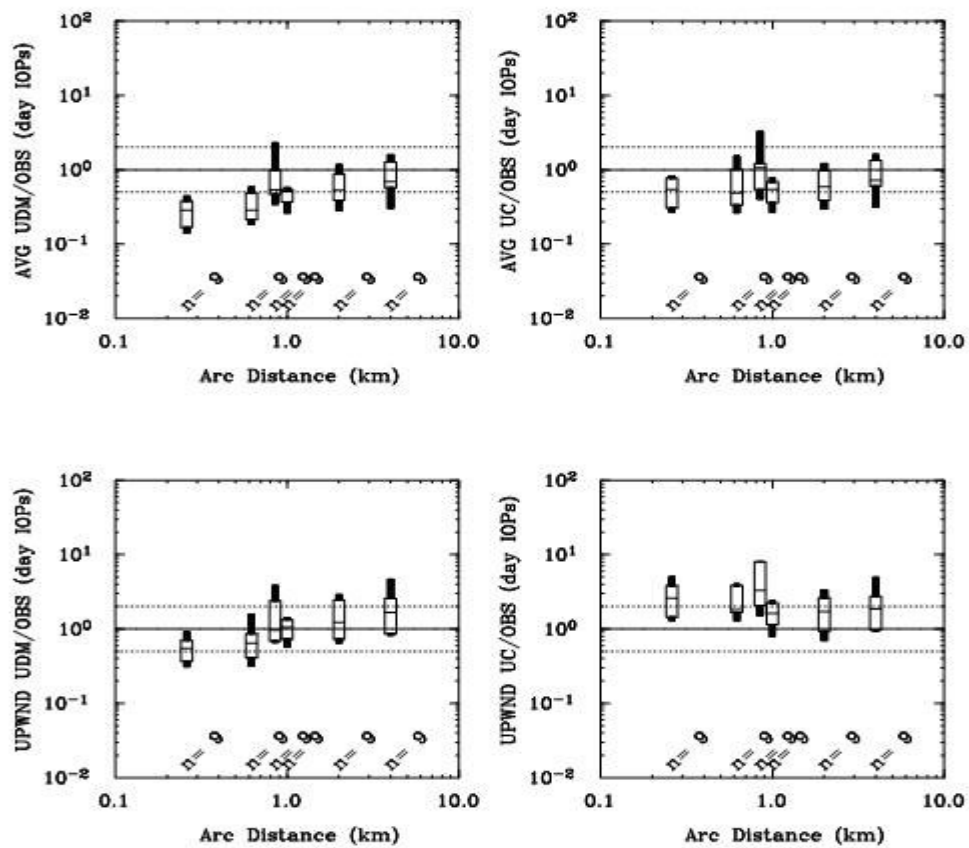


Figure 8. Residual plots (X_p/X_o vs x) of arc max concentrations, C_{max} , for HPAC urban options UDM and UC with Average (AVG) (top) and Upwind (UPWIND) (bottom) meteorological inputs, for day IOPs. The significant lines on the box plots indicate, from bottom to top, the 2th, 16th, 50th (i.e., the median), 84th, and 98th percentiles of the n X_p/X_o points at that arc distance.

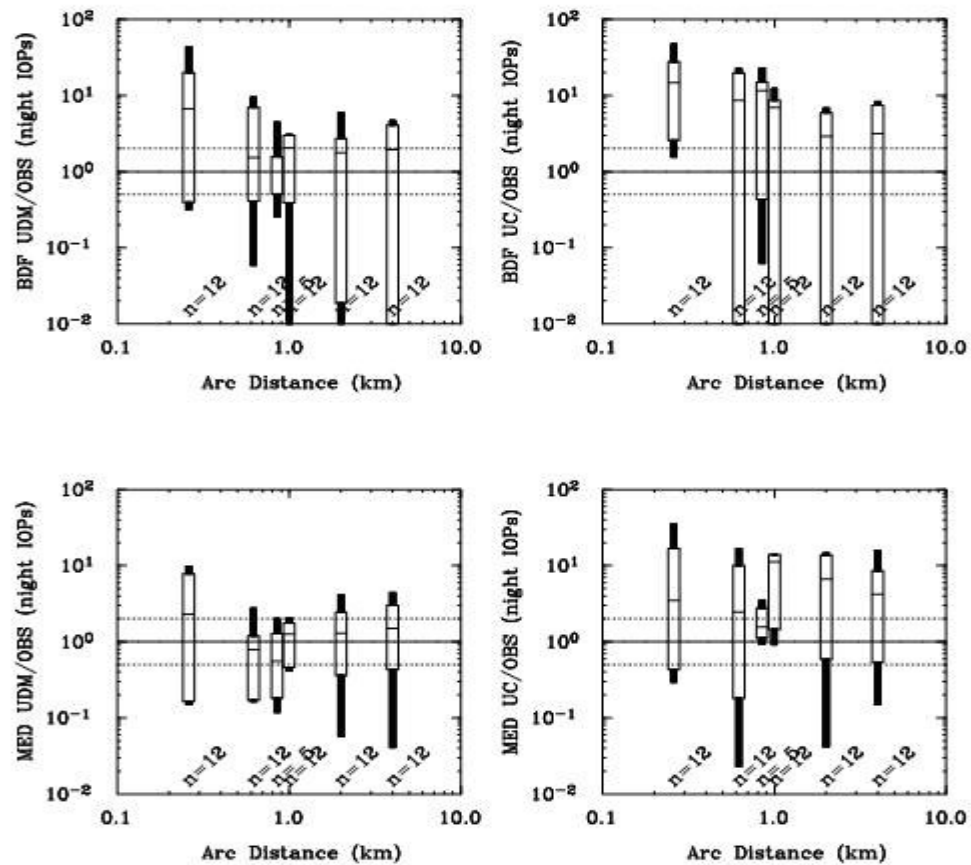


Figure 9. Residual plots (X_p/X_o vs x) of arc max concentrations, C_{max} , for HPAC urban options UDM and UC with Basic Default (BDF) (top) and MM5 MEDOC (bottom) meteorological inputs, for night IOPs. The significant lines on the box plots indicate, from bottom to top, the 2th, 16nd, 50th (i.e., the median), 84th, and 98th percentiles of the n X_p/X_o points at that arc distance.

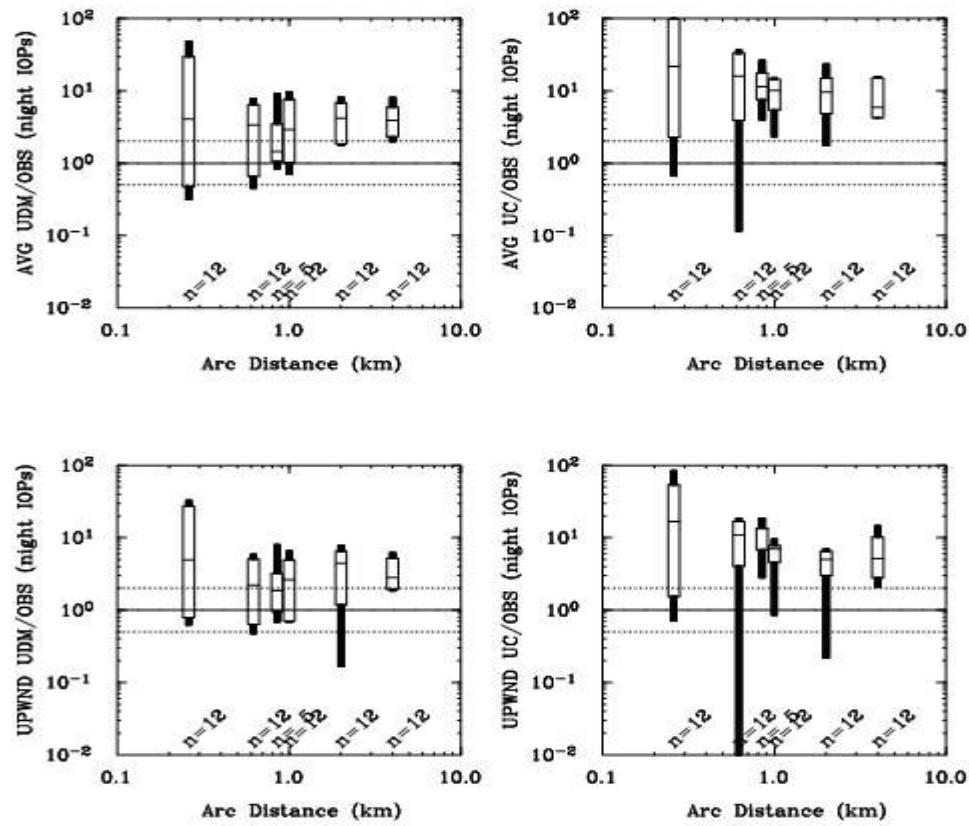


Figure 10. Residual plots (X_p/X_o vs x) of arc max concentrations, C_{max} , for HPAC urban options UDM and UC with Average (AVG) (top) and Upwind (UPWIND) (bottom) meteorological inputs, for night IOPs. The significant lines on the box plots indicate, from bottom to top, the 2th, 16nd, 50th (i.e., the median), 84th, and 98th percentiles of the n X_p/X_o points at that arc distance.

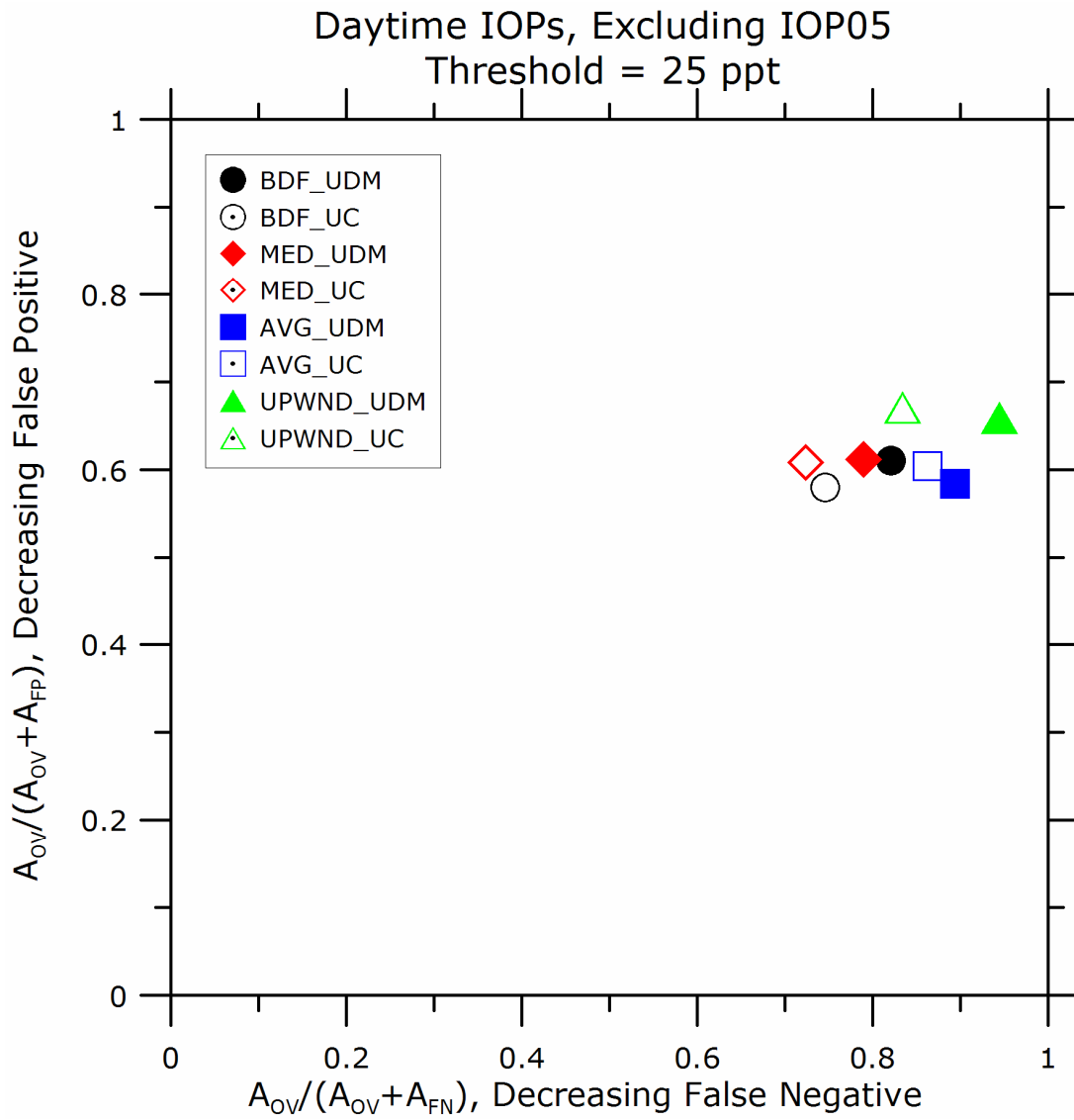


Figure 11. Plot of MOE_{FP} versus MOE_{FN} for the daytime IOPs, excluding IOP05. The different points represent the two different urban model options (UC and UDM) and the four different meteorological input options. A threshold of 25 ppt is assumed.

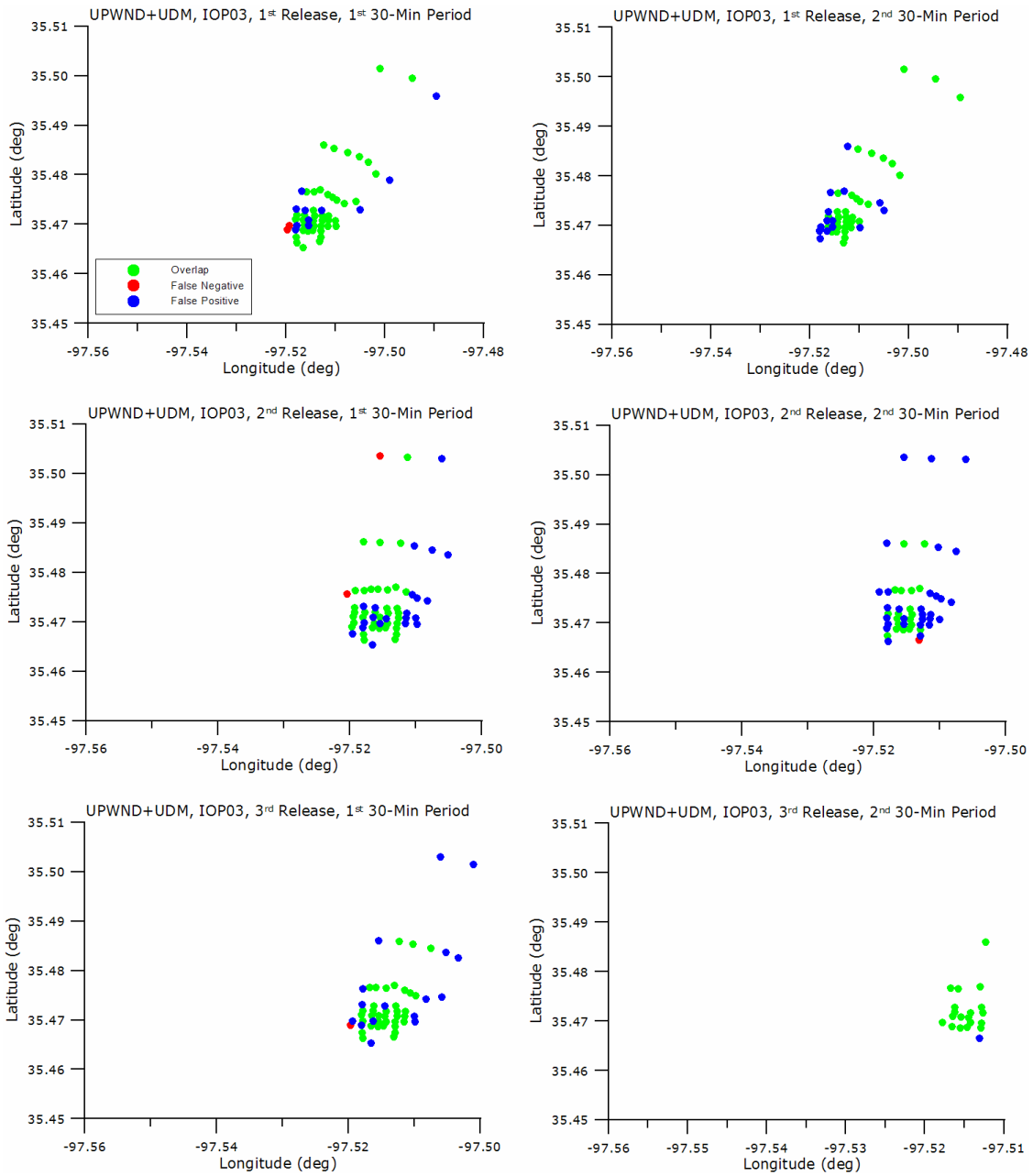


Figure 12. The first two 30-min periods for each of three releases during IOP03 are plotted. The figures show significant samplers based on an SF₆ threshold of 25 ppt and HPAC predictions given by the UPWIND met option and UDM model option. The dots in the figures are colored according to the following convention: “Green” samplers: both observations and predictions are above 25 ppt (overlap), “Red” samplers: observations above and predictions below 25 ppt (false negative), “Blue” samplers: observations below and predictions above 25 ppt (false positive). Samplers where both observations and predictions are below 25 ppt are not shown.

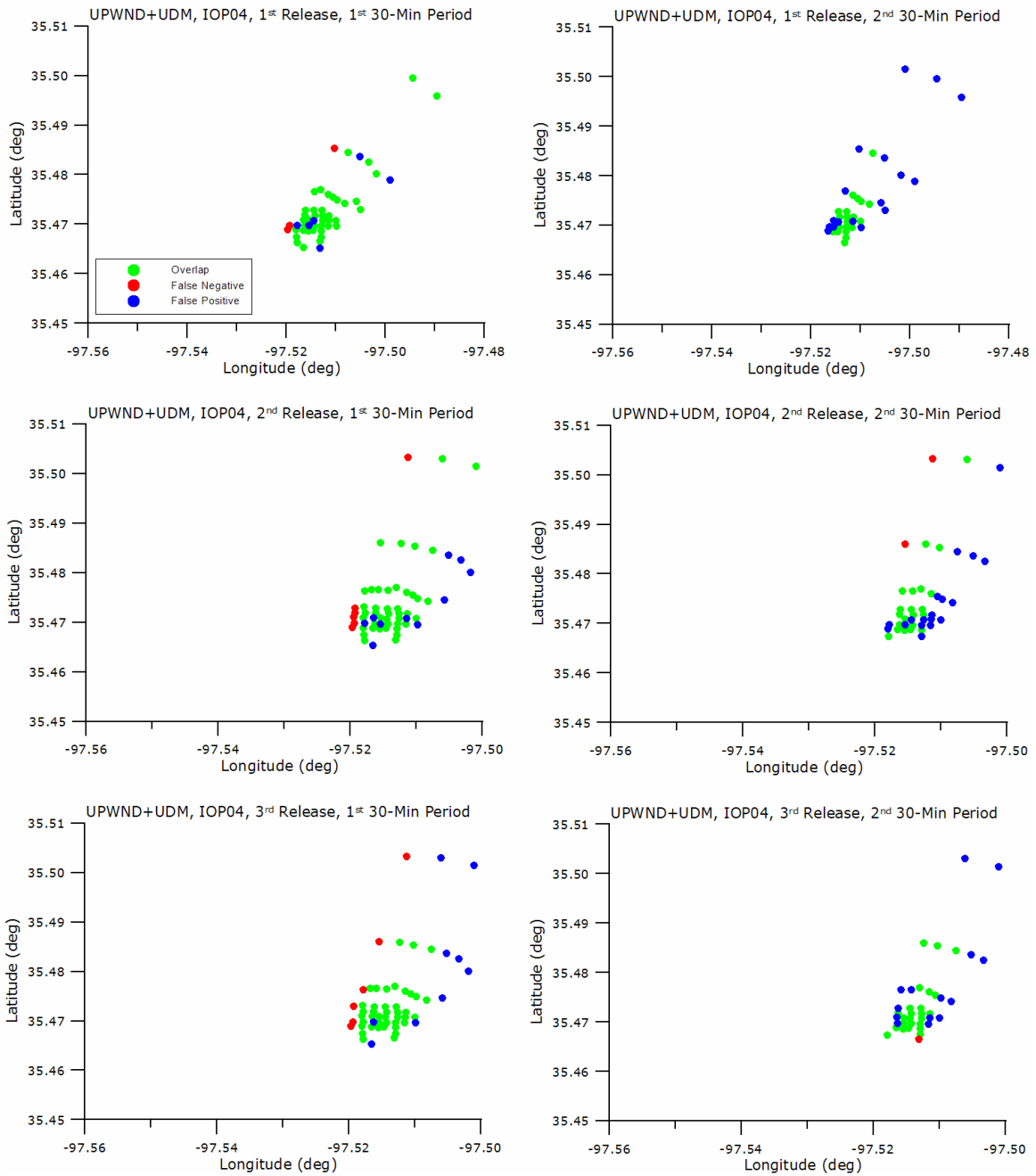


Figure 13. The first two 30-min periods for each of three releases during IOP04 are plotted. The figures show significant samplers based on an SF₆ threshold of 25 ppt and HPAC predictions given by the UPWIND met option and UDM model option. The dots in the figures are colored according to the following convention: “Green” samplers: both observations and predictions are above 25 ppt (overlap), “Red” samplers: observations above and predictions below 25 ppt (false negative), “Blue” samplers: observations below and predictions above 25 ppt (false positive). Samplers where both observations and predictions are below 25 ppt are not shown.

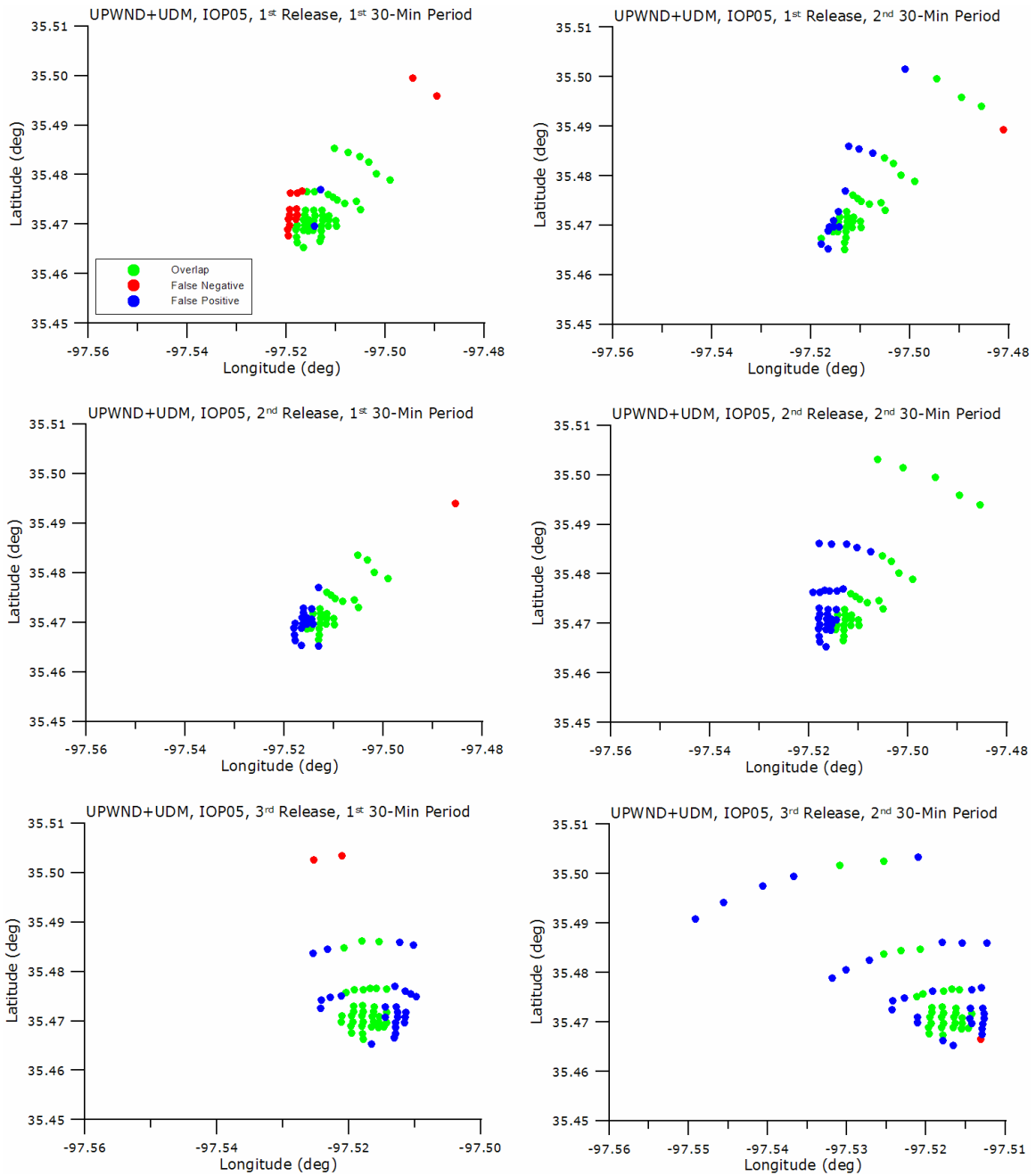


Figure 14. The first two 30-min periods for each of three releases during IOP05 are plotted. The figures show significant samplers based on an SF₆ threshold of 25 ppt and HPAC predictions given by the UPWIND met option and UDM model option. The dots in the figures are colored according to the following convention: “Green” samplers: both observations and predictions are above 25 ppt (overlap), “Red” samplers: observations above and predictions below 25 ppt (false negative), “Blue” samplers: observations below and predictions above 25 ppt (false positive). Samplers where both observations and predictions are below 25 ppt are not shown.

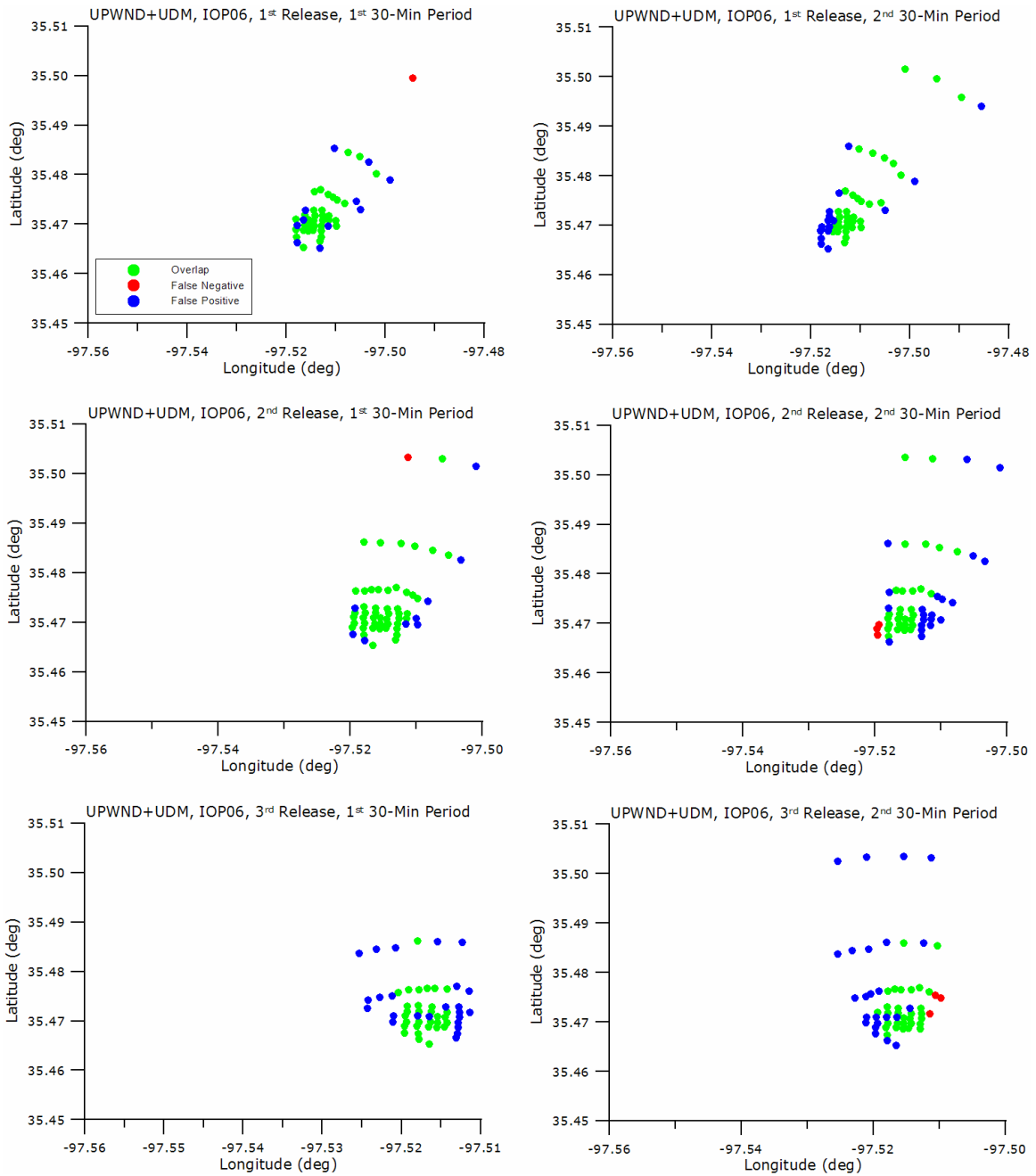


Figure 15. The first two 30-min periods for each of three releases during IOP06 are plotted. The figures show significant samplers based on an SF₆ threshold of 25 ppt and HPAC predictions given by the UPWIND met option and UDM model option. The dots in the figures are colored according to the following convention: “Green” samplers: both observations and predictions are above 25 ppt (overlap), “Red” samplers: observations above and predictions below 25 ppt (false negative), “Blue” samplers: observations below and predictions above 25 ppt (false positive). Samplers where both observations and predictions are below 25 ppt are not shown.

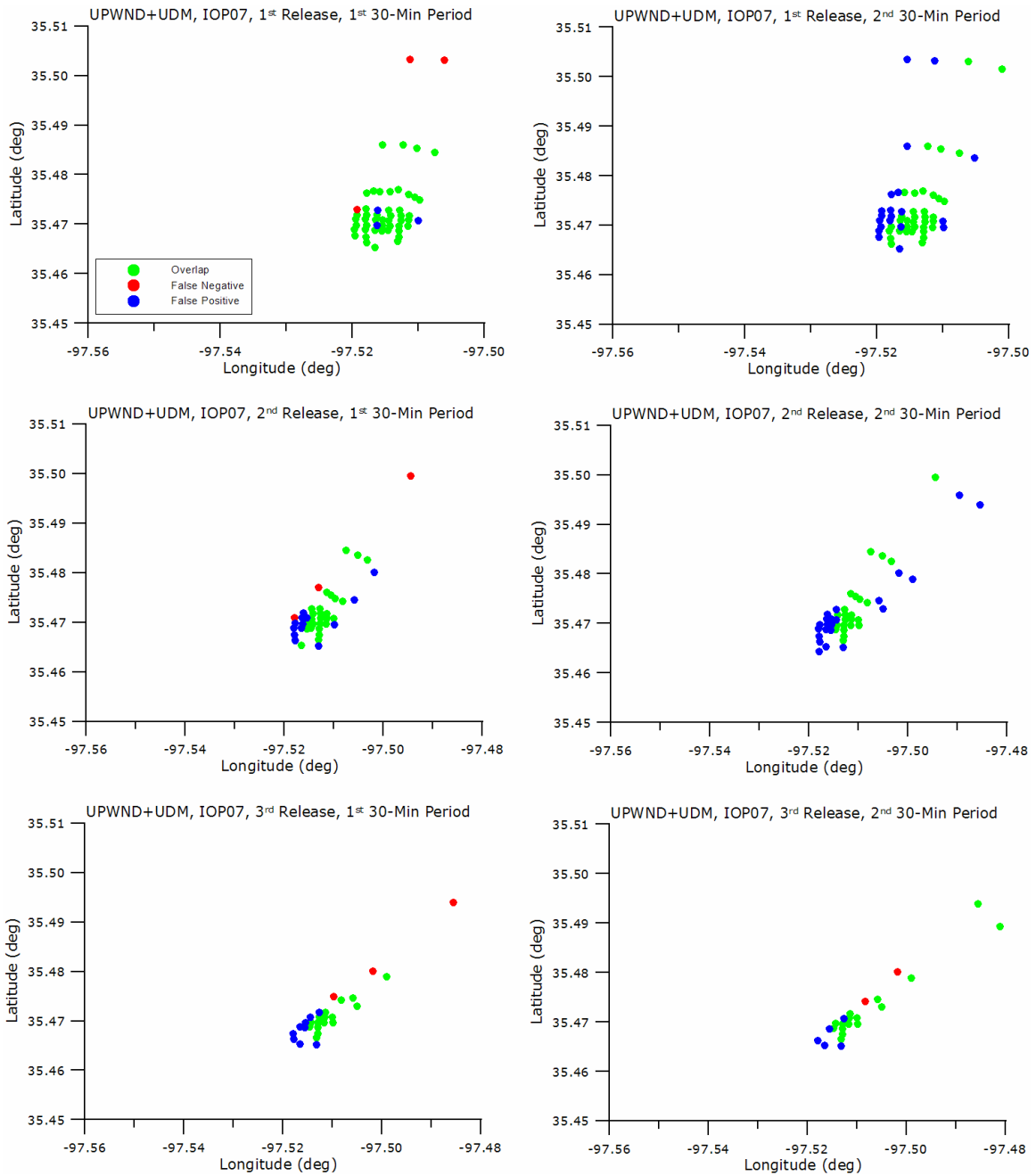


Figure 16. The first two 30-min periods for each of three releases during IOP07 are plotted. The figures show significant samplers based on an SF₆ threshold of 25 ppt and HPAC predictions given by the UPWIND met option and UDM model option. The dots in the figures are colored according to the following convention: “Green” samplers: both observations and predictions are above 25 ppt (overlap), “Red” samplers: observations above and predictions below 25 ppt (false negative), “Blue” samplers: observations below and predictions above 25 ppt (false positive). Samplers where both observations and predictions are below 25 ppt are not shown.

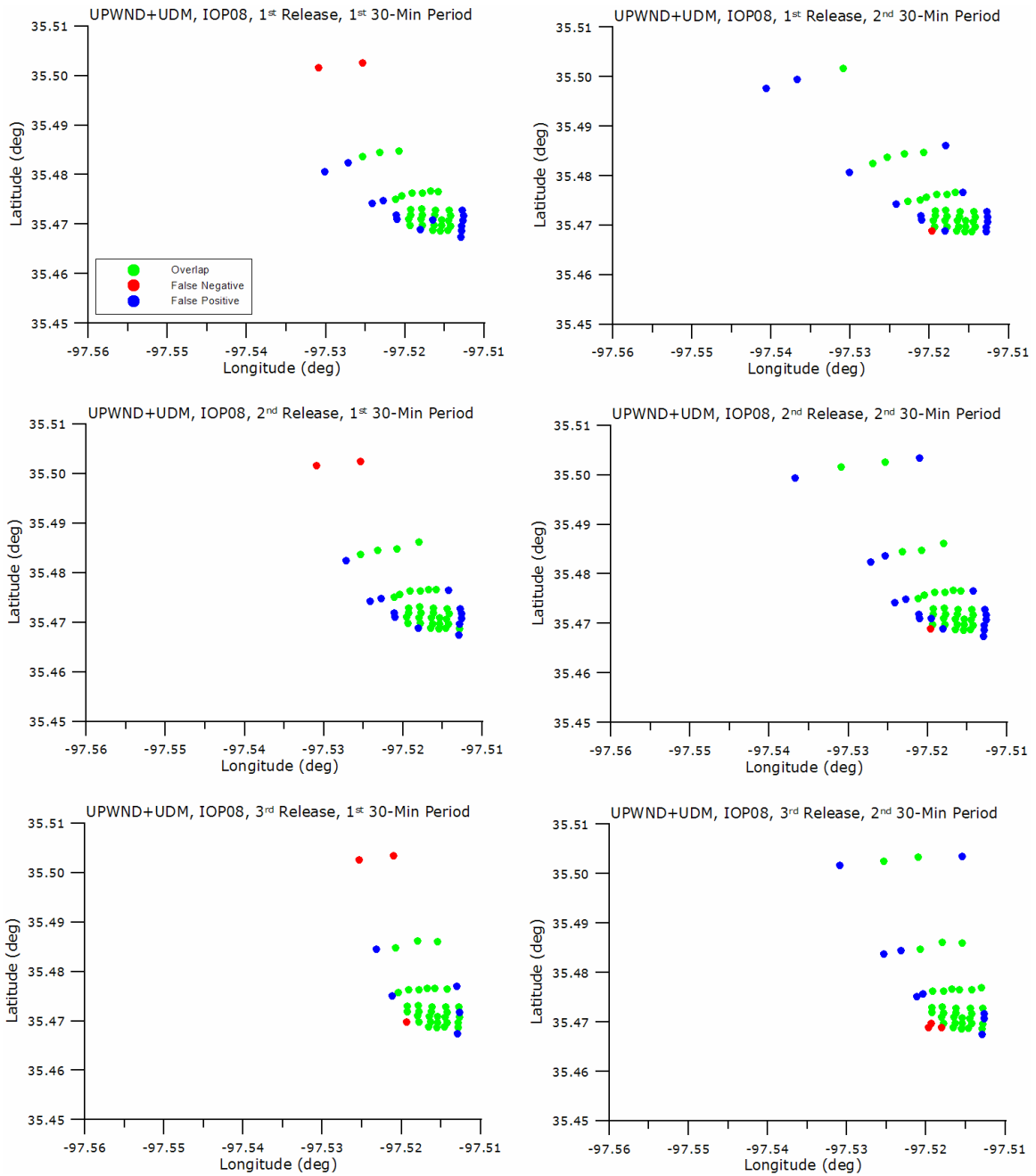


Figure 17. The first two 30-min periods for each of three releases during IOP08 are plotted. The figures show significant samplers based on an SF₆ threshold of 25 ppt and HPAC predictions given by the UPWIND met option and UDM model option. The dots in the figures are colored according to the following convention: “Green” samplers: both observations and predictions are above 25 ppt (overlap), “Red” samplers: observations above and predictions are below 25 ppt (false negative), “Blue” samplers: observations below and predictions above 25 ppt (false positive). Samplers where both observations and predictions are below 25 ppt are not shown.

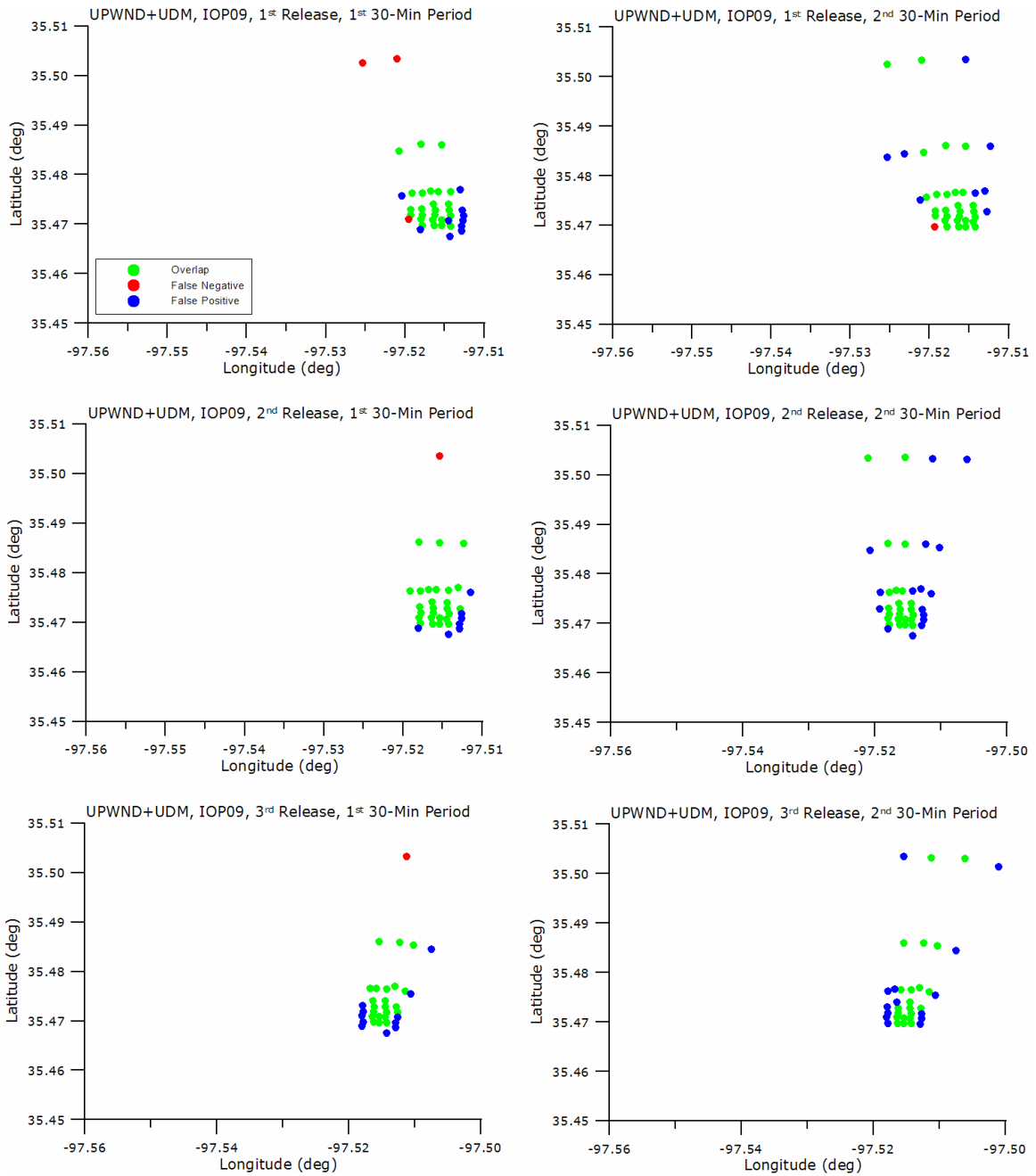


Figure 18. The first two 30-min periods for each of three releases during IOP09 are plotted. The figures show significant samplers based on an SF₆ threshold of 25 ppt and HPAC predictions given by the UPWIND met option and UDM model option. The dots in the figures are colored according to the following convention: “Green” samplers: both observations and predictions are above 25 ppt (overlap), “Red” samplers: observations above and predictions below 25 ppt (false negative), “Blue” samplers: observations below and predictions above 25 ppt (false positive). Samplers where both observations and predictions are below 25 ppt are not shown.

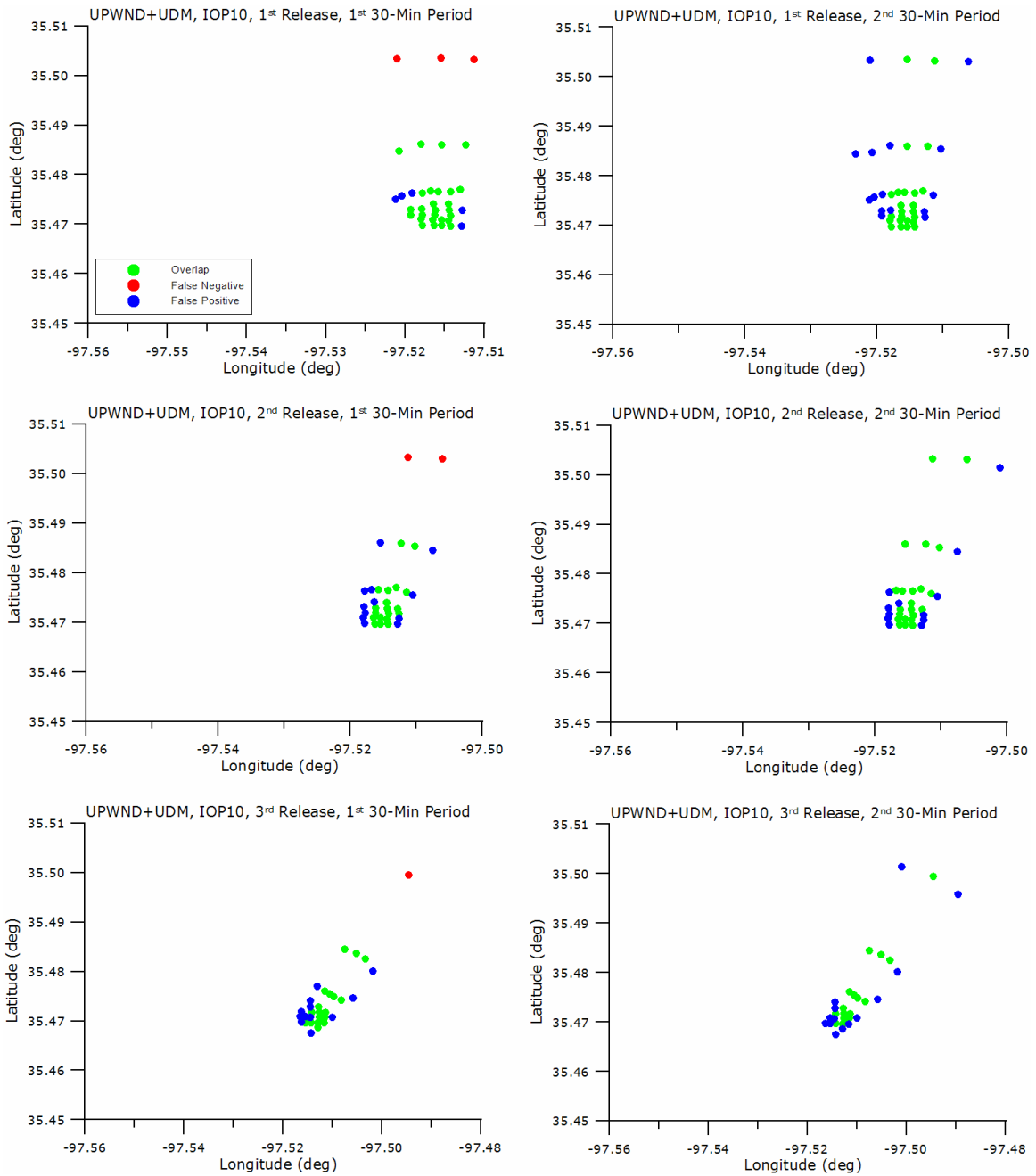


Figure 19. The first two 30-min periods for each of three releases during IOP10 are plotted. The figures show significant samplers based on an SF₆ threshold of 25 ppt and HPAC predictions given by the UPWIND met option and UDM model option. The dots in the figures are colored according to the following convention: “Green” samplers: both observations and predictions are above 25 ppt (overlap), “Red” samplers: observations above and predictions below 25 ppt (false negative), “Blue” samplers: observations below and predictions above 25 ppt (false positive). Samplers where both observations and predictions are below 25 ppt are not shown.